Biochemical and Biophysical Research Communications 450 (2014) 283–288

Contents lists available at ScienceDirect

Biochemical and Biophysical Research Communications

journal homepage: www.elsevier.com/locate/ybbrc

Tetrameric ZBRK1 DNA binding domain has affinity towards cognate DNA in absence of zinc ions

Lumbini R. Yadav, Mahamaya N. Biswal, Vikrant, M.V. Hosur, Ashok K. Varma *

Advanced Centre for Treatment, Research and Education in Cancer, Kharghar, Navi Mumbai, Maharashtra 410 210, India

ARTICLE INFO

Article history:
Received 12 May 2014
Available online 9 June 2014

Keywords:
ZBRK1
Zinc-finger
Oligomer
Secondary structure

ABSTRACT

Zinc finger transcription regulatory proteins play crucial roles in cell-cycle regulation, DNA damage response and tumor genesis. Human ZBRK1 is a zinc-finger transcription repressor protein, which recognizes double helical DNA containing consensus sequences of 5′GGGXXXCAGXXXTTT3′. In the present study, we have purified recombinant DNA binding domain of ZBRK1, and studied binding with zinc ions and DNA, using biophysical techniques. The elution profile of the purified protein suggests that this ZBRK1 forms a homotetramer in solution. Dissociation and pull down assays also suggest that this domain forms a higher order oligomer. The ZBRK1-DNA binding domain acquires higher stability in the presence of zinc ions and DNA. The secondary structure of the ZBRK1-DNA complex is found to be significantly altered from the standard B-DNA conformation.

1. Introduction

Zinc finger proteins, are known to play pivotal roles, through transcriptional regulation in DNA replication and repair, protein translation, cell proliferation and apoptosis. Regulation of gene expression using customized transcription factors has been reported recently [1,2]. Chimeric ZF proteins have been engineered to obtain customized activities, such as restriction, methylation and integration [3,4]. The erb2 oncogene and peripheral arterial obstructive diseases have been repressed by customized ZF proteins [5]. ZF proteins contain more than one ZF in tandem, and are considered potential targets for drugs. They can also make the genome a potential drug target.

There are different types of ZF proteins, and these are classified based on the environment around zinc ions. The major class is the C2H2 class, which contains a consensus amino acid sequence ψ-X-Cys-X(2–4)-Cys-X3-ψ-X5-ψ-X2-His-X(3,4)-His, where X is any amino acid and ψ is any hydrophobic residue. C2H2 type containing the KRAB (Kruppel-associated box) domain forms the largest subfamily (KRAB-ZFP) of ZF proteins [6] and, ZBRK1 is a member of this family. Human ZBRK1 performs a variety of biological functions through its various domains: the N-terminal KRAB, eight consecutive central C2H2 zinc fingers and a BRCA1-dependent C-terminal transcriptional repression domain (CTRD) [7]. ZBRK1 consists of 532 amino acids, and the region from residues 206 to 424 is the DNA-binding domain (DBD). The N-terminal KRAB domain also performs repressor function by interacting with other proteins, such as KAP1. ZBRK1 represses cellular invasion and metastasis and, its loss enhances MMP9 transcription in cervical cancer [8]. ZBRK1 represses a high mobility group AT-hook 2 (HMGA2), a DNA architectural protein, activation of which plays a significant role in tumor genesis and metastasis [9]. The repressor ZBRK1 binds to a 15 bp consensus nucleotide sequence, GGGXXXCAGXXXTTT (where X is any nucleotide), which is found near promoter regions of many DNA damage inducible genes like p21, ANG1 [10] GADD153 and GADD45 [11,12]. Exposure of cells to DNA damaging agents leads to degradation of ZBRK1 via the BRCA1-independent ubiquitin–proteasome pathway leading to de-repression [13]. Interaction of ZBRK1 with Trim28 and histone deacetylase, results in repression of HIV-1 LTR acting as an intrinsic retroviral defense system [14]. In order to understand the various functions of ZBRK1, in details, we have initiated to study the structure and interactions of ZBRK1 with different ligands.

Here, we report purification and biophysical characterization of the DNA binding domain of ZBRK1 (ZBRK1-DBD), and an analysis of its binding with zinc and the cognate oligonucleotide. It is found that this domain exists as a homotetramer in solution, in contradiction to earlier report that C-terminal residues were essential for tetramer formation [15]. ZBRK1-DBD binds only to double

Abbreviations: CD, circular dichroism spectroscopy; ZBRK1, zinc finger and BRCA1-interacting protein with a KRAB domain 1; ZF, zinc-finger.

* Corresponding author. Fax: +91 22 2740 5085.
E-mail address: avarma@actrec.gov.in (A.K. Varma).

http://dx.doi.org/10.1016/j.bbrc.2014.05.104
0006-291X/

stranded DNA, even in the absence of zinc ions. The DNA is found to be overwound on binding, while the conformation of the protein becomes less compact.

2. Materials and methods

2.1. Reagents

All the enzymes used for cloning were procured from NEB (US). Oligonucleotides were ordered from Sigma Aldrich (US). Chemicals used were from HiMedia, Qualigens and Sigma Aldrich. Bacterial culture media, IPTG and ampicillin were from HiMedia (India).

2.2. Cloning of ZBRK1-DNA binding domain

ZBRK1-DBD from amino acid 206 to 424 was sub-cloned at the BamHI and HinDIII site in pRSET-A vector (Invitrogen). Forward primer 5′-GTCTCCGAGAACCTGTACTTTCAG GGTTGTGTGCAGTGAA TGTGGGAA-3′ and Reverse primer 5′-GTCAAGCTTCT ATTAGTGTAT TCTCTTATGCTTAAC-3′ were used for polymerase chain reaction. The forward primer has TEV site incorporated in it so as to enable cleavage of the native protein from histidine tag. The ligated samples were transformed into *Escherichia coli* DH5α cells and plated on ampicillin plates. Ampicillin resistant colonies were screened for positive clones and correct DNA sequence (Genetic Analyser-Applied Bio Systems).

2.3. Protein expression and purification

E. coli bacterial strain Rosetta 2(DE3) (Invitrogen) was transformed with ZBRK1-DBD construct. Single colony was inoculated in Luria Bertani broth containing ampicillin (100 μg/ml) and chloramphenicol (34 μg/ml), and the culture was allowed to grow for 12–14 h. Cells were then diluted 100 fold and grown till the OD_{600} reached a value of 0.7. This culture was then induced with 0.4 mM IPTG for 16 h at 18 °C. Cells were harvested and resuspended in buffer-A containing 10 mM HEPES pH 7.0, 500 mM NaCl, 0.1% Triton X-100, 20 mM β-ME, 1 mM EDTA, 2.5% glycerol, and 10 mM imidazole. Cells were lysed by sonication at a pulse rate of 50, three times with 1 min duty cycle. Cell debris was removed by centrifugation. Cell lysis was allowed to bind on Ni–NTA resin for 1–2 h at 25 °C. To remove the nonspecifically bound protein, resin was washed with buffer-A addition containing 50 mM imidazole. Fusion protein was eluted with imidazole (500 and 750 mM) and further treated with TEV protease to remove histidine tag.

2.4. Gel filtration chromatography

ZBRK1-DBD was further purified to homogeneity using AKTA explorer system (GE Healthcare). Concentrated protein was chromatographed using Superdex-75 column pre equilibrated with buffer (5 mM HEPES pH 7.0, 150 mM NaCl, and 20 mM β-mercaptoethanol). Four proteins (BSA, lysozyme, phosphorylase B, and carbonic anhydrase) were eluted from the same column under similar conditions to prepare the standard plot for molecular weight estimation. The sample was run at a flow rate of 0.5 ml/min, and 1 ml fractions were collected. FPLC purified protein was further passed through buffer exchange column to remove β-mercaptoethanol. Peptide mass fingerprinting was done for protein confirmation using MALDI-MS (Ultraflex Bruker Daltonics system).

2.5. MBP pull down assay

MBP-ZBRK1ΔK and MBP were expressed and affinity purified using amylose resin. Purified ZBRK1-DBD was incubated with MBP-ZBRK1ΔK and MBP for 3 h on ice with gentle mixing. Amylose resin was washed with buffer-A to remove non-specifically bound ZBRK1-DBD. The resin was then loaded on 12% SDS gel to check for the pull down.

2.6. Circular dichroism spectroscopy

Far UV CD scan of ZBRK1-DBD (7 μM) was monitored to study secondary structural characteristics. Scan was recorded from 240 to 190 nm at a scanning speed of 20 nm/min, data interval of 0.1 nm and 3 accumulations. To study the effect of zinc sulfate and DNA on secondary structural characteristics, ZBRK1-DBD was titrated with zinc sulfate (10–180 μM) and DNA (5–30 μM). To reveal the structural alteration in DNA due to ZBRK1 binding, CD scan was obtained from 300 to 200 nm at a scanning speed of 20 nm/min. Protein concentration was estimated directly by Bradford method assuming a molar extinction coefficient of 12,950 M^{-1} cm^{-1}. All the spectra were measured at 25 °C using (Jasco J-815) spectropolarimeter, and were baseline corrected. α-Helical content of the protein was estimated using ellipticity signals at 208 and 222 nm and the standard equation [16].

2.7. Thermal stability

To measure the thermal stability of ZBRK1-DBD (5 μM), CD spectra in the range 250–200 nm was recorded as a function of temperature. Far UV CD scan was monitored at every 5 °C increase in temperature, with an equilibration time of 3 min and a scanning speed of 50 nm/min. Thermal unfolding pathway was also studied to reveal the effect of $ZnSO_4$ (0.1 mM) and DNA (30 μM) on the stability of ZBRK1-DBD. Ellipticity at 222 nm was plotted as a function of temperature to understand the course of change in secondary structure elements.

2.8. Fluorescence spectroscopy

Spectrofluorometer (JOBIN YVON Horiba Fluorolog 3) was used for fluorescence measurements. The emission slit width was 5 nm. The fluorescence scan was measured in the emission wavelength range of λ_{em} 310–500 nm, and the excitation was at 295 nm. The spectral data were collected using FluorESSENCE software. Protein concentration was measured using molar extinction coefficient as described before. Titration experiments with ZBRK1-DBD and different concentrations of DNA (4–60 μM) and $ZnSO_4$ (5–110 μM) were performed to study the tertiary structural alterations.

2.9. Isothermal titration calorimetry (ITC)

ZBRK1-DBD (50 μM) was injected into calorimetric cell containing buffer to study the heat effects from dissociation. Thirteen injections each 3 μl, were injected at 25 °C, allowing an equilibration time of 150 s between injections. Interaction studies of ZBRK1-DBD with $ZnSO_4$ and consensus double stranded DNA oligonucleotide (5′GGGACGCAGTTTTAT3′) were performed using MicroCal iTC200 calorimeter. (GE Healthcare) The titration experiments were done under following conditions: (1) 5.2 μM of ZBRK-DBD in cell and 1 mM of $ZnSO_4$ in syringe, (2) 20 μM of ZBRK1-DBD in cell and 200 μM of DNA in syringe. Protein concentration was estimated, using BSA as standard.

3. Results

3.1. Expression and purification of ZBRK1-DBD

Two liters of bacterial culture yielded 0.4 mg of >95% of pure ZBRK1-DBD protein (Fig. 1A). A single band corresponding to a

molecular weight of 24 kDa suggests that the preparation is very homogeneous. Peptide mass fingerprinting further confirmed the sample to be ZBRK1-DBD (data not shown).

3.2. ZBRK1-DBD forms a tetramer

ZBRK1-DBD eluted at approximately 58 ml from 16/60 Superdex75 size exclusion column (Fig. 1B). This indicates that the protein forms a higher order oligomer. From the standard linear graph of $\log_{10}$ (molecular weight) versus (elution volume), the size of the eluted sample was estimated to be approximately 94 kDa (Fig. 1B). The partition coefficient Kav, for ZBRK1-DBD was calculated from the elution volume [17,18]. Stoke's radius of ZBRK1-DBD was interpolated from a plot of partition coefficient (Kav) versus Stoke's radii for standard markers. The calculated Stoke's radius of ZBRK1-DBD was 5.6 nm which is closer to Stoke's radius of standard of 97 kDa. To explore the ability of self-association of ZBRK1-DBD, MBP pull down assay with MBP tagged ZBRK1ΔK construct was performed. ZBRK1-DBD showed interaction with ZBRK1ΔK construct. No interaction was visible with MBP (Fig. 1C).

Thus, based on size exclusion chromatography and pull down assay, it is proposed that the ZBRK1-DBD forms a homotetramer in solution.

To confirm the formation of an oligomer, next we performed dissociation study using ITC. Addition of concentrated protein from the syringe into calorimeter cell containing the buffer-resulted in a heat change, which gradually decreased as concentration of the protein inside the cell increased (Fig. 1D). This observation suggests that the heat change was due to dissociation of an oligomeric species. The dissociation curve yielded enthalpy of dissociation as −482 kcal/mol with a dissociation constant of 0.125 μM.

3.3. Secondary structure alterations on ligand binding

Far UV CD spectrum of ZBRK1-DBD is shown in (Fig. 2A). The scan showed peaks at approximately 222, 208 and 195 nm, which are characteristic of alpha-helical conformation [16,19]. The alpha-helical content of ZBRK1-DBD, estimated using measured ellipticities at 222 and 208 nm, was 12% and 15% respectively. The CD spectra of ZBRK1-DBD were recorded at different concentrations of zinc (Fig. 2B) and DNA (Fig. 2C). The $\theta_{222}/\theta_{208\,nm}$ ratio of only protein is 1.0, and this ratio increases with further addition of $ZnSO_4$, indicating incorporation of quaternary structure. In the case of interaction with DNA, this ratio decreased, indicating reduction in coiled coil structure [16,20]. Fig. 2D shows the CD spectrum over the λ range of 320–230 nm, when DNA was titrated with varying

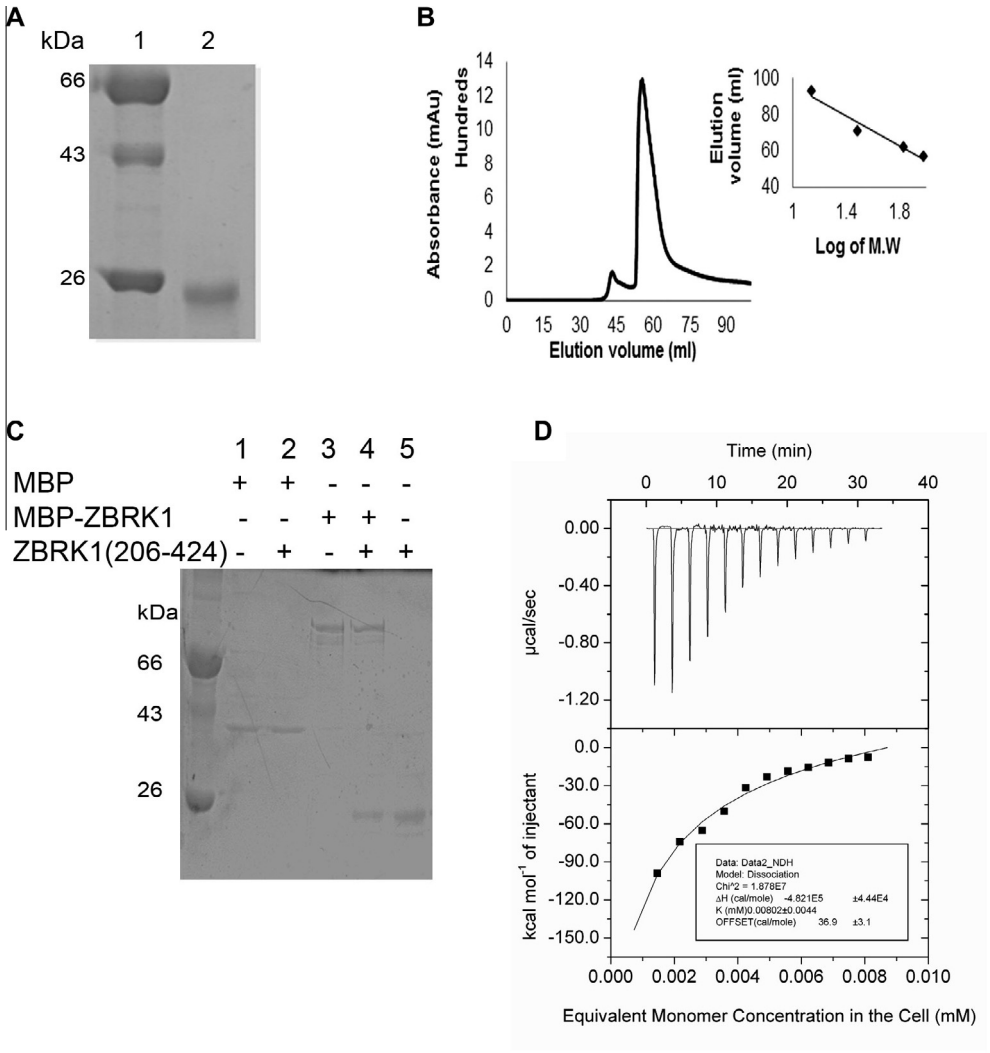

Fig. 1. Oligomeric characterization of ZBRK1-DBD: (A) size exclusion chromatography profile of purified ZBRK1-DBD protein. Inset is a plot of log of molecular weight standards (carbonic anhydrase, lysozyme, phosphorylase B and BSA) vs. elution volumes. (B) SDS electrophoresis showing sample purity. (C) MBP pull-down (lanes 1, 3, 5 – show input), (lane 2, 4 – pull down samples). (D) Exothermic heat pulses for 3 μl injections into buffer of ZBRK1-DBD (50 μM). Lower panel shows integrated heat data after blank correction.

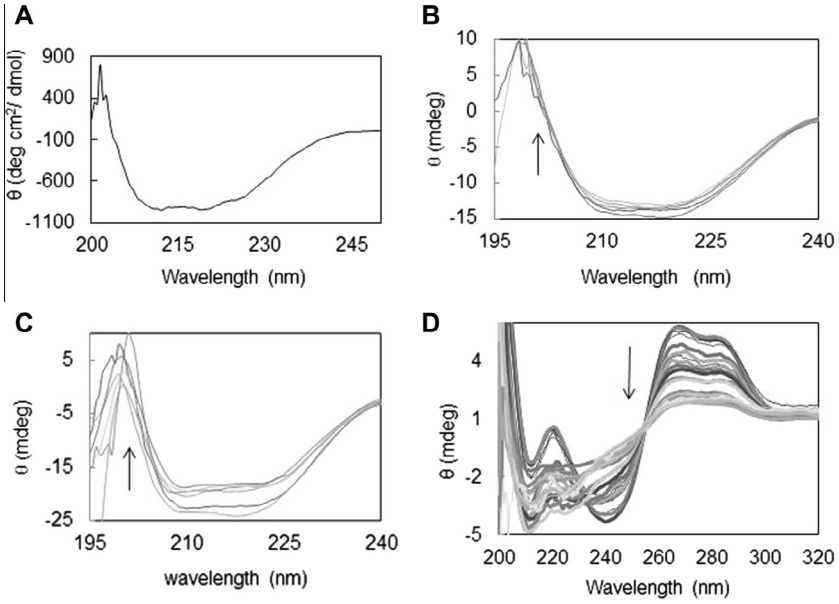

Fig. 2. CD spectra: (A) ZBRK1-DBD. ZBRK1-DBD titrated with (B) DNA, (C) zinc sulfate. (D) DNA titrated with ZBRK1-DBD. Arrows indicate directions of decrease in ellipticity.

amounts of ZBRK1-DBD. The CD spectrum of B-form DNA is composed of four major peaks: negative peaks around 214 and 245 nm and positive peaks around 225 and 280 nm [21,22]. The positive maximum around 280 nm is attributed to base stacking and the negative peak at 245 nm is attributed to DNA helicity [23]. The changes in ellipticities at 275 nm and 245 nm, on addition of ZBRK1-DBD, indicate that the standard B-geometry of the DNA is being altered by protein binding.

3.4. Intrinsic tryptophan fluorescence to elucidate local tryptophan environment

Tryptophan emission spectrum recorded from 310 to 500 nm, upon excitation at 295 nm (supplemental Fig. 1A). Emission maximum observed at 336 nm indicates that the single tryptophan residue is in hydrophobic environment [24]. Titration of ZBRK1-DBD with DNA (supplemental Fig. 1B) and zinc sulfate (supplemental Fig. 1C) showed a decrease in fluorescence intensity without any shift in the position of the maxima. This suggests that interaction of ZBRK1-DBD with either zinc sulfate or with DNA does not have any effect on local tryptophan environment.

3.5. Thermal stability

To evaluate the nature of folding and unfolding transitions, and to measure the structural stability of ZBRK1-DBD in presence of DNA and $ZnSO_4$ the far UV CD spectra, were recorded at different temperatures (Fig. 3). Variation in the ellipticity at 222 nm as a function of temperature suggests that ZBRK1-DBD unfolds via three state unfolding transitions with T_m values of 58 and 69 °C. Presence of zinc sulfate or DNA with ZBRK1 increased thermal stability of protein as suggested by increases in melting temperatures from 57 °C to 62 °C and 68 °C, respectively. Interestingly, in the presence of either DNA or zinc sulfate, ZBRK1 demonstrated simply two state unfolding transitions.

3.6. Thermodynamics of ligand binding to ZBRK1-DBD

Fig. 4 shows the results of calorimetry experiments to study the interactions of ZBRK1 with zinc sulfate and DNA. Model fitting for ZBRK1-DBD with zinc sulfate with one set of sites showed

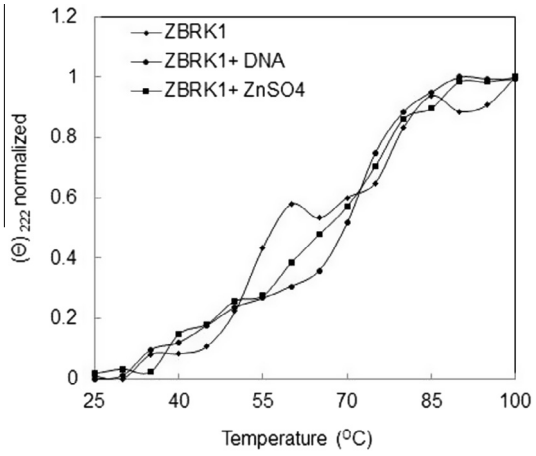

Fig. 3. Thermal denaturation profile of ZBRK1-DBD. Plot of fraction unfolded versus temperature at 5 °C intervals.

exothermic reaction with a stoichiometry of 1:42. It demonstrated an affinity of 1.4 μM under these conditions (Fig. 4A). Nonlinear curve fitting done using one set of sites for ZBRK1-DBD with DNA demonstrated a stoichiometry of 1:2 with binding affinity of 0.29 μM (Fig. 4B). ZBRK1-DBD interaction with zinc sulfate and DNA is an enthalpically driven reaction. Thermodynamic parameters of protein interaction with zinc and DNA, derived from ITC experiments are tabulated (Table 1).

4. Discussion

4.1. Oligomeric DBD

The elution profile of ZBRK1-DBD from the gel filtration column clearly indicates that ZBRK1-DBD was a homotetramer in solution. The absence of any substantial monomeric peak implies a very high affinity for tetramer formation. MBP pull down assay also revealed the ability of ZBRK1-DBD to oligomerize with ZBRK1ΔK in the MBP tagged ZBRK1ΔK construct. The ITC titration also suggests that dissociation of ZBRK1-DBD is enthalpically favored.

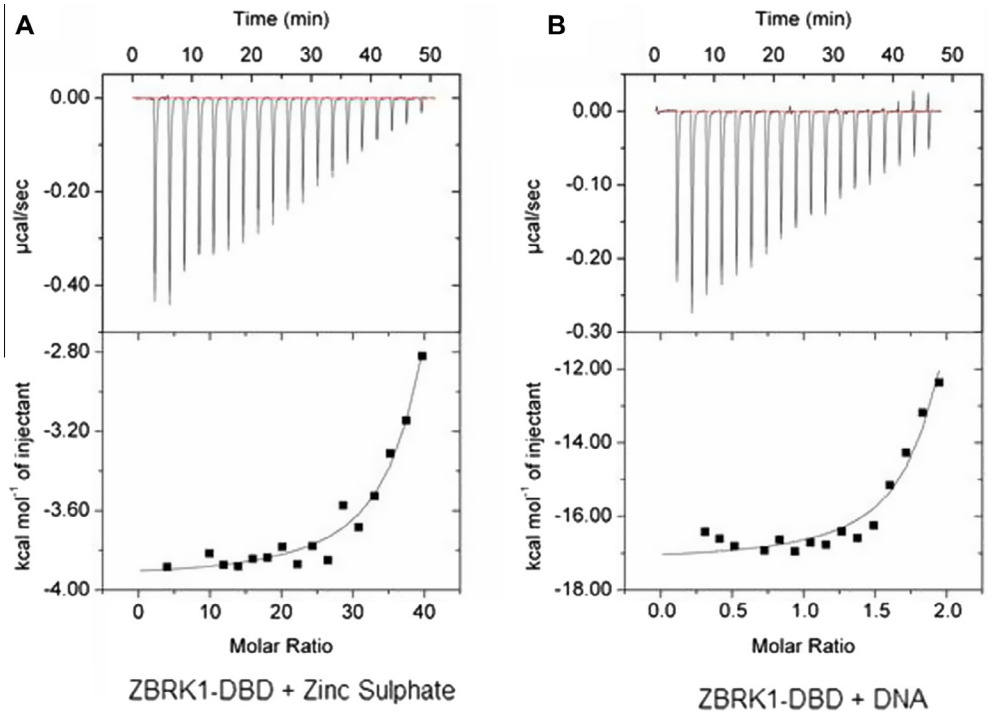

Fig. 4. Interaction of ZBRK1-DBD with: (A) zinc sulfate (B) DNA.

Table 1
Thermodynamic parameters derived from heat change: ZBRK1-DBD interaction with (1) zinc sulfate, (2) DNA.

	$ZnSO_4$	DNA
Interaction model	One set of sites	One set of sites
N sites	42.9 ± 0.0817	2.1 ± 0.0538
K_d (µm)	1.4	0.29
K (M^{-1})	7.06E5 ± 1.91E5	3.44E6 ± 1.26E6,
ΔH (cal/mol)	−3927 ± 29.88	−1.714E4 ± 192.6
ΔS (cal/mol/deg)	13.4	−27.6
Chi^2 value	3510	1.34E + 05

The negative enthalpy change of dissociation implies that association process will be endothermic and entropically driven. The presence of two transitions in thermal unfolding pathway is also consistent with presence of tetrameric species. The first transition with a T_m of 58 °C would be for the disassembly of the tetramer, while the second transition with a T_m of 68 °C would be for denaturation of the monomers. The stoichiometry of 1:42 for zinc binding of ZBRK1-DBD, containing eight zinc fingers is also supportive for tetrameric oligomerisation of ZBRK1-DBD (Table.1). Tetramer formation has also been established by chemical cross-linking experiments [15]. However, in these studies, the molecule was full length ZBRK1ΔK construct, and not just the DNA binding domain used here. In fact experiments conducted by these authors with a variety of C-terminal deletion constructs show that, C-terminal nine residues are absolutely essential for formation of stable tetramers. Against this background our observation that ZBRK1-DBD, which lacks 108 residues from the C-terminal region, is a homo tetramer in solution, is a very novel finding. It is conceivable that the nature of tetramers formed by full length ZBRK1 and ZBRK1-DBD are different. The biological implications of this observation are not yet clear. Tetrameric DNA-binding proteins are known. The transcription factor p53 forms a tetramer. One dimer part of the tetramer binds to half site of consensus DNA sequence & the binding of second dimer to the other half enhances the affinity to DNA almost 50-fold [25]. Mutations in the mostly hydrophobic residues responsible for tetramerization can inactivate the wild type protein suggesting the importance of tetramerization in p53 function [26] OB fold proteins that bind single stranded DNA are tetrameric [27,28]. Bioinformatics and EMSA analysis, however, shows that ZBRK1-DBD does not have the OB fold and does not bind ss DNA. (data not shown).

4.2. Zinc ions for DNA binding

The DNA-binding motif in ZF proteins comprises of two beta strands and an alpha helix, and the amino acid residues from the helix bind a triplet of bases in the major groove of the DNA helix [29–31]. Formation of the helix and proper positioning of the helical residues for optimal interaction is assumed to be ensured by coordination of zinc ion to conserved cysteine and histidine residues of the motif [32]. Therefore Zn ions are essential for repressor activity of C2H2 type of zinc fingers [33]. Interestingly, in the present study, ZBRK1-DBD binds to 15 bp consensus DNA sequence even in the absence of Zn ions (Fig. 2D, supplemental Fig. 1B). EMSA (data not shown) and ITC (Fig. 4A) also revealed interaction in absence of Zn ions.

4.3. DNA and protein conformation

It has been observed that the structure of DNA bound by ZF protein is altered from the standard B-geometry [34]. Molecular modeling has revealed that this distortion is necessitated by the requirement for neighboring fingers to bind optimally in the major groove. The actual distortions observed in the crystal structures of complexes are in agreement with predictions by modeling experiments. [35]. The relative intensity of CD signal at 275 nm is often taken as a signature for DNA geometry. An increase in its intensity suggests unwinding of DNA and/or displacement of base-pairs away from helix axis. However, in the present study on ZBRK1-DBD: DNA complex, the CD signals at 275 nm is significantly decreased. The geometry of the DNA in the complex is likely to be over wound compared to B-DNA. This probably may help ZBRK1

in repression activity, on interaction with DNA. Although previous reports mention no change occurs in ZF conformation on DNA binding, our results indicate subtle changes. Interestingly, binding of Zn and DNA to ZBRK1-DBD appear to have opposite effects on protein conformation. The n–$\pi*$ transition at 220 nm in CD reflects the α-helical content. The π–$\pi*$ excitation band at 208 nm is sensitive to whether the α-helix is involved in tertiary contacts [36]. The ratio $\theta_{222}/\theta_{208\,nm}$ is, therefore, regarded as an indicator of quaternary structure through inter-α-helix coiling/interaction. The binding of protein to DNA (Fig. 2C) suggests decrease in $\theta_{222}/\theta_{208\,nm}$ ratio indicating decrease in compactness of protein. On the other hand, ZBRK1-DBD with Zn ions indicated increase in $\theta_{222}/\theta_{208\,nm}$ ratio (Fig. 2B) suggesting incorporation of quaternary structure in presence of Zn as compared to Zn deficient protein.

In conclusion, our report indicates that ZBRK1-DBD forms tetramer. ZBRK1-DBD binds exclusively to double stranded DNA with stoichiometry of 1:2, even in the absence of zinc ions. Interaction of ZBRK1-DBD with $ZnSO_4$ and DNA leads to higher thermal stability. In the complex with ZBRK1-DBD, the DNA is distorted from standard B-geometry. The future goal of this work is to crystallize the protein for understanding the structure, which will help in using it as a drug target and also to engineer it for therapeutic purposes.

Acknowledgments

We thank Dr. Thomas G. Boyer, University of Texas Health Science Center at San Antonio, Texas, USA for MBP-ZBRK1ΔK construct. MVH thanks DAE for the award of Raja Ramanna Fellowship. AKV thanks TMC-ACTREC for funding.

Appendix A. Supplementary data

Supplementary data associated with this article can be found, in the online version, at http://dx.doi.org/10.1016/j.bbrc.2014.05.104.

References

[1] H.S. Zhang, D. Liu, Y. Huang, S. Schmidt, R. Hickey, D. Guschin, H. Su, I.S. Jovin, M. Kunis, S. Hinkley, Y. Liang, L. Hinh, S.K. Spratt, C.C. Case, E.J. Rebar, B.E. Ehrlich, P.D. Gregory, F.J. Giordano, A designed zinc-finger transcriptional repressor of phospholamban improves function of the failing heart, Mol. Ther. 20 (2012) 1508–1515.
[2] A. Klug, Towards therapeutic applications of engineered zinc finger proteins, FEBS Lett. 579 (2005) 892–894.
[3] F.D. Bushman, M.D. Miller, Tethering human immunodeficiency virus type 1 preintegration complexes to target DNA promotes integration at nearby sites, J. Virol. 71 (1997) 458–464.
[4] R.R. Beerli, B. Dreier, C.F. Barbas 3rd, Positive and negative regulation of endogenous genes by designed transcription factors, Proc. Natl. Acad. Sci. U.S.A. 97 (2000) 1495–1500.
[5] P.Q. Liu, E.J. Rebar, L. Zhang, Q. Liu, A.C. Jamieson, Y. Liang, H. Qi, P.X. Li, B. Chen, M.C. Mendel, X. Zhong, Y.L. Lee, S.P. Eisenberg, S.K. Spratt, C.C. Case, A.P. Wolffe, Regulation of an endogenous locus using a panel of designed zinc finger proteins targeted to accessible chromatin regions. Activation of vascular endothelial growth factor A, J. Biol. Chem. 276 (2001) 11323–11334.
[6] M.F. Rousseau-Merck, D. Koczan, I. Legrand, S. Moller, S. Autran, H.J. Thiesen, The KOX zinc finger genes: genome wide mapping of 368 ZNF PAC clones with zinc finger gene clusters predominantly in 23 chromosomal loci are confirmed by human sequences annotated in EnsEMBL, Cytogenet. Genome Res. 98 (2002) 147–153.
[7] L. Zheng, H. Pan, S. Li, A. Flesken-Nikitin, P.L. Chen, T.G. Boyer, W.H. Lee, Sequence-specific transcriptional corepressor function for BRCA1 through a novel zinc finger protein, ZBRK1, Mol. Cell 6 (2000) 757–768.
[8] L.F. Lin, C.H. Chuang, C.F. Li, C.C. Liao, C.P. Cheng, T.L. Cheng, M.R. Shen, J.T. Tseng, W.C. Chang, W.H. Lee, J.M. Wang, ZBRK1 acts as a metastatic suppressor by directly regulating MMP9 in cervical cancer, Cancer Res. 70 (2010) 192–201.
[9] T. Ahmed, S.M. Kelly, N.C. Price, A.J. Lawrence, Activation of phospholipase A(2) by long chain fatty acyl groups involves a novel unstable linkage, J. Biochem. 127 (2000) 871–875.
[10] S. Furuta, J.M. Wang, S. Wei, Y.M. Jeng, X. Jiang, B. Gu, P.L. Chen, E.Y. Lee, W.H. Lee, Removal of BRCA1/CtIP/ZBRK1 repressor complex on ANG1 promoter leads to accelerated mammary tumor growth contributed by prominent vasculature, Cancer Cell 10 (2006) 13–24.
[11] W. Tan, L. Zheng, W.H. Lee, T.G. Boyer, Functional dissection of transcription factor ZBRK1 reveals zinc fingers with dual roles in DNA-binding and BRCA1-dependent transcriptional repression, J. Biol. Chem. 279 (2004) 6576–6587.
[12] V. Garcia, J.M. Garcia, C. Pena, J. Silva, G. Dominguez, R. Rodriguez, C. Maximiano, R. Espinosa, P. Espana, F. Bonilla, The GADD45, ZBRK1 and BRCA1 pathway: quantitative analysis of mRNA expression in colon carcinomas, J. Pathol. 206 (2005) 92–99.
[13] J. Yun, W.H. Lee, Degradation of transcription repressor ZBRK1 through the ubiquitin–proteasome pathway relieves repression of Gadd45a upon DNA damage, Mol. Cell. Biol. 23 (2003) 7305–7314.
[14] H. Nishitsuji, M. Abe, R. Sawada, H. Takaku, ZBRK1 represses HIV-1 LTR-mediated transcription, FEBS Lett. 586 (2012) 3562–3568.
[15] W. Tan, S. Kim, T.G. Boyer, Tetrameric oligomerization mediates transcriptional repression by the BRCA1-dependent Kruppel-associated box-zinc finger protein ZBRK1, J. Biol. Chem. 279 (2004) 55153–55160.
[16] S.M. Kelly, N.C. Price, The use of circular dichroism in the investigation of protein structure and function, Curr. Protein Pept. Sci. 1 (2000) 349–384.
[17] F. Wolfram, E. Morris, C.W. Taylor, Three-dimensional structure of recombinant type 1 inositol 1,4,5-trisphosphate receptor, Biochem. J. 428 (2010) 483–489.
[18] C. Dulac, A.A. Michels, A. Fraldi, F. Bonnet, V.T. Nguyen, G. Napolitano, L. Lania, O. Bensaude, Transcription-dependent association of multiple positive transcription elongation factor units to a HEXIM multimer, J. Biol. Chem. 280 (2005) 30619–30629.
[19] R.W. Woody, Circular dichroism, Methods Enzymol. 246 (1995) 34–71.
[20] T. Rao, G. Ruiz-Gomez, T.A. Hill, H.N. Hoang, D.P. Fairlie, J.M. Mason, Truncated and helix-constrained peptides with high affinity and specificity for the cFos coiled-coil of AP-1, PLoS One 8 (2013) e59415.
[21] M. Vorlickova, Conformational transitions of alternating purine–pyrimidine DNAs in perchlorate ethanol solutions, Biophys. J. 69 (1995) 2033–2043.
[22] J. Kypr, M. Vorlickova, Circular dichroism spectroscopy reveals invariant conformation of guanine runs in DNA, Biopolymers 67 (2002) 275–277.
[23] C.A. Sprecher, W.A. Baase, W.C. Johnson Jr., Conformation and circular dichroism of DNA, Biopolymers 18 (1979) 1009–1019.
[24] R.W. Alston, L. Urbanikova, J. Sevcik, M. Lasagna, G.D. Reinhart, J.M. Scholtz, C.N. Pace, Contribution of single tryptophan residues to the fluorescence and stability of ribonuclease Sa, Biophys. J. 87 (2004) 4036–4047.
[25] K.G. McLure, P.W. Lee, How p53 binds DNA as a tetramer, EMBO J. 17 (1998) 3342–3350.
[26] P. Chène, The role of tetramerization in p53 function, Oncogene 20 (2001).
[27] S. Raghunathan, C.S. Ricard, T.M. Lohman, G. Waksman, Crystal structure of the homo-tetrameric DNA binding domain of *Escherichia coli* single-stranded DNA-binding protein determined by multiwavelength X-ray diffraction on the selenomethionyl protein at 2.9-A resolution, Proc. Natl. Acad. Sci. U.S.A. 94 (1997) 6652–6657.
[28] D.L. Theobald, R.M. Mitton-Fry, D.S. Wuttke, Nucleic acid recognition by OB-fold proteins, Annu. Rev. Biophys. Biomol. Struct. 32 (2003) 115–133.
[29] S.A. Wolfe, L. Nekludova, C.O. Pabo, DNA recognition by Cys2His2 zinc finger proteins, Annu. Rev. Biophys. Biomol. Struct. 29 (2000) 183–212.
[30] D. Lu, C2H2 zinc-finger recognition of biomolecules, Yao Xue Xue Bao 48 (2013) 834–841.
[31] P.V. Pedone, R. Ghirlando, G.M. Clore, A.M. Gronenborn, G. Felsenfeld, J.G. Omichinski, The single Cys2-His2 zinc finger domain of the GAGA protein flanked by basic residues is sufficient for high-affinity specific DNA binding, Proc. Natl. Acad. Sci. U.S.A. 93 (1996) 2822–2826.
[32] R.N. De Guzman, H.Y. Liu, M. Martinez-Yamout, H.J. Dyson, P.E. Wright, Solution structure of the TAZ2 (CH3) domain of the transcriptional adaptor protein CBP, J. Mol. Biol. 303 (2000) 243–253.
[33] E.E. Zheleznova, J.H. Crosa, R.G. Brennan, Characterization of the DNA- and metal-binding properties of *Vibrio anguillarum* fur reveals conservation of a structural Zn(2+) ion, J. Bacteriol. 182 (2000) 6264–6267.
[34] L. Nekludova, C.O. Pabo, Distinctive DNA conformation with enlarged major groove is found in Zn-finger-DNA and other protein–DNA complexes, Proc. Natl. Acad. Sci. U.S.A. 91 (1994) 6948–6952.
[35] M. Elrod-Erickson, M.A. Rould, L. Nekludova, C.O. Pabo, Zif268 protein-DNA complex refined at 1.6 A: a model system for understanding zinc finger-DNA interactions, Structure 4 (1996) 1171–1180.
[36] N.E. Zhou, C.M. Kay, R.S. Hodges, Synthetic model proteins. Positional effects of interchain hydrophobic interactions on stability of two-stranded alpha-helical coiled-coils, J. Biol. Chem. 267 (1992) 2664–2670.